EDGE ARTICLE

Check for updates

Mechanochemical generation of acid-degradable poly(enol ether)s†

Jinghui Yang [ID] and Yan Xia [ID] *

In an effort to develop polymers that can undergo extensive backbone degradation in response to mechanical stress, we report a polymer system that is hydrolytically stable but unmasks easily hydrolysable enol ether backbone linkages when force is applied. These polymers were synthesized by ring-opening metathesis polymerization (ROMP) of a novel mechanophore monomer consisting of cyclic ether fused bicyclohexene. Hydrogenation of the resulting polymers led to significantly enhanced thermal stability (T_d > 400 °C) and excellent resistance toward acidic or basic conditions. Solution ultrasonication of the polymers resulted in up to 65% activation of the mechanophore units and conversion to backbone enol ether linkages, which then allowed facile degradation of the polymers to generate small molecule or oligomeric species under mildly acidic conditions. We also achieved solid-state mechano-activation and polymer degradation *via* grinding the solid polymer. Force-induced hydrolytic polymer degradability can enable materials that are stable under force-free conditions but readily degrade under stress. Facile degradation of mechanically activated polymechanophores also facilitates the analysis of mechanochemical products.

Introduction

Polymer mechanochemistry explores the use of mechanical force to direct selective chemical transformations in force-responsive molecules called mechanophores.[1,2] Embedding properly designed mechanophores in polymer backbones can induce nondestructive covalent bond transformations and generate materials with a wide range of force-responses.[3–11] Mechanical activation of mechanophores is usually accompanied by nonselective chain scission, and chain scission can halt further activation of mechanophores.[12] While it has long been known that high molecular weight (MW) polymers undergo undesired mechanical degradation under shear stress,[13,14] mechanically triggered chemical degradation over an extended strand of polymer (rather than a single-point chain degradation) is an interesting and desired mechanical response. It can enhance the extent of polymer degradation to result in much smaller species. Such polymers may enable effective self-destruction and minimize their environmental impact. For fundamental study of mechanochemistry, incorporating force-triggered degradable units in polymechanophores may facilitate the analysis of the mechanochemical products and provide

information on the continuity (or discontinuity) of poly-mechanophore activation.

In 2020, the Craig and Wang groups simultaneously reported strategies for mechanically "unlocking" polymer degradability by fusing hydrolysable lactone and cyclic ketal linkages with cyclobutane mechanophores in the polymer backbone. Upon ring-opening of cyclobutane, these hydrolysable moieties become backbone linkages and enable hydrolytic degradation of the mechanochemically activated polymers (Scheme 1A and B).[15,16] Subsequently, the Craig group reported a clever alternative design of a tetrasubstituted [4.2.0]bicyclooctene based mechanophore that, upon mechanochemical ring-opening into 1,3-cyclo-octadiene, can spontaneously undergo intramolecular lactonization and result in backbone cleavage (Scheme 1C).[17] These recent examples showcased mechanically enhanced polymer degradation as a new modality of response, but in these designs, the hydrolysable functionalities already exist in the polymers before mechanoactivation. As a result, deleterious hydrolysis prior to the desired mechanoactivation would inevitably hydrolyze these same functionalities in the precursor polymers and change their properties, leading to the generation of undesired scissile cyclobutane linkages or premature polymer cleavage that disrupts the transduction of force and thus limits the extent of mechanoactivation. We herein report a new design of polymechanophores that overcomes these limitations and only contains completely chemically inert linkages, but upon mechanoactivation, easily hydrolysable and degradable linkages are unmasked. Taking advantage of the olefins generated from mechanochemical ring-opening of cyclobutane, we sought to

Department of Chemistry, Stanford University, Stanford, California, 94305, USA. E-mail: yanx@stanford.edu

† Electronic supplementary information (ESI) available: Detailed descriptions of synthetic procedures, ^{1}H and ^{13}C NMR spectra of new compounds, GPC traces and single crystal structure. Crystallographic data for compound **S2**. CCDC 2023034. For ESI and crystallographic data in CIF or other electronic format see DOI: 10.1039/d1sc00001b

A. Craig 2020:
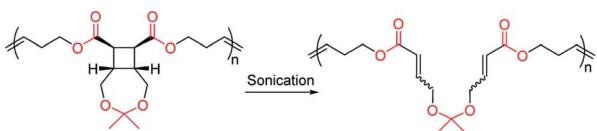
## B. Wang 2020:
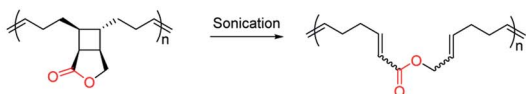
C. Craig 2020:
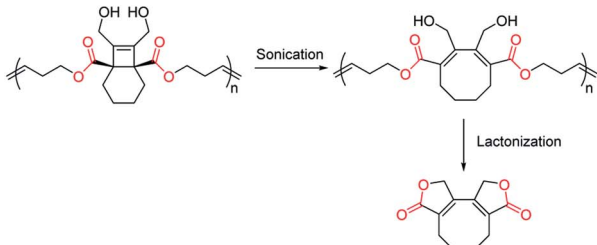
D. This Work:
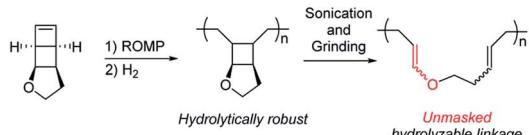
Scheme 1 Designs of polymers that can mechanochemically generate degradable backbone linkages.

mechanically convert chemically inert alkyl ether linkages to acid-labile enol ether linkages. The resultant poly(enol ether)s can be rapidly degraded under mildly acidic conditions but remain stable under basic conditions.[18–20]

Results and discussions

We have developed a general strategy to directly polymerize mechanophore monomers in a controlled fashion to generate polymechanophores, and designed such polymechanophores to undergo dramatic mechanochemical transformation from non-conjugated structures to conjugated structures.[21–24] Leveraging this strategy, we designed a tricyclic mechanophore monomer **1**
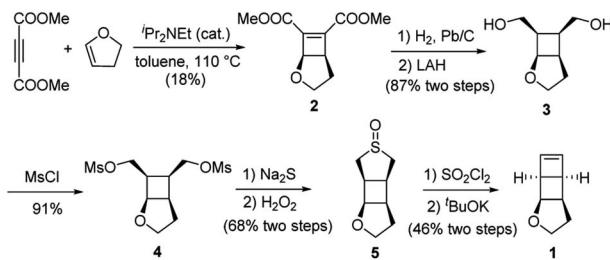
Scheme 2 Synthesis of monomer **5**.

that can be synthesized from commercially available chemicals at gram scales as outlined in Scheme 2. Thermally induced [2 + 2] cycloaddition between dimethyl acetylenedicarboxylate and 2,3-dihydrofuran produced bicyclic compound **2**,[25] which was subsequently hydrogenated and reduced to afford diol **3**. **3** was found to have an exclusive *endo* configuration (Fig. S1†) due to the high facial selectivity in the hydrogenation step. Treatment of **3** with MsCl afforded dimesylate **4**, which was then treated with Na$_2$S followed by oxidation with H$_2$O$_2$ to yield sulfoxide **5**. Chlorination of **5** by one equivalent of SO$_2$Cl$_2$ generated α-chlorosulfoxide as a mixture of different regioisomers and stereoisomers, which underwent sulfoxide Ramberg–Bäckland olefination to generate **1** as a volatile liquid.

The ring opening metathesis polymerization (ROMP) of **1** was then explored using the fast-initiating Grubbs catalyst **G3**. **G3** was added into a solution of **1** in CHCl$_3$ ([**1**]$_0$ = 1 M) at room temperature with a target degree of polymerization (DP) of 1000. ^{1}H NMR analysis of the crude reaction mixture indicated complete monomer conversion within 15 min. Despite the fast polymerization, gel permeation chromatography (GPC) of the polymerization solution showed an asymmetric peak skewed to the low MW side and the measured MW was lower than the expected value (Fig. S2†). We have previously observed reduced stability of the propagating Ru in ROMP of ladderenes, but the stability is improved at lower temeratures.[22] Delightfully, lowering the polymerization temperature to 0 °C yielded a symmetric peak with expected MW and low dispersity. The
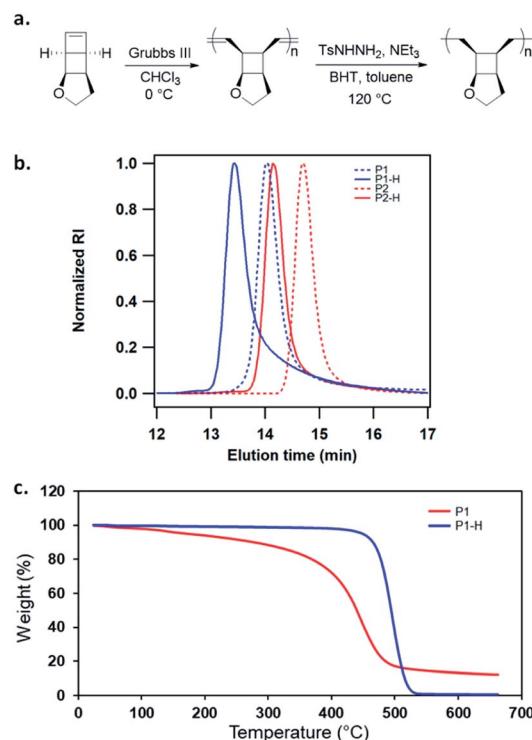

Fig. 1 (a) ROMP of monomer **1** and subsequent hydrogenation (the specified stereochemistry refers to that of the repeat unit, not suggesting the polymer tacticity). (b) GPC traces of poly(**1**) at different DPs and their hydrogenated polymers. (c) TGA traces of poly(**1**) and hydrogenated poly(**1**).

Table 1 Summary of synthesized polymers

Polymer	DP_{theory}	$M_{n,theory}$ (kDa)	$M_{n,MALLS}$[a] (kDa)	Đ
P1	1000	122	121	1.14
P2	500	61.1	63.1	1.04
P3	1000[b]	186	172	1.10
P1-H	1000	124	141	1.17
P2-H	500	62.1	74.0	1.10
P3-H	1000[b]	188	179	1.13

[a] Determined by GPC MALLS analysis in THF. [b] Equal composition of **1** and **NBE-EtHex**.

measured MWs agreed with the theoretical values and could be controlled by the ratio of $[1]_0/[G3]_0$ (**P1** and **P2** in Fig. 1b and Table 1). However, if the quenched polymer solution was left under ambient conditions, low MW polymers were progressively formed over a few hours (Fig. S3†), suggesting decomposition of the ROMP polymer. Differential scanning calorimetry (DSC) analysis of the isolated ROMP polymer showed two overlapping irreversible exothermic peaks starting from 46 °C (Fig. S4†). The limited thermal stability was also corroborated by thermogravimetric analysis (TGA), which showed gradual mass loss starting from ∼100 °C (Fig. 1c). To probe the thermal decomposition, poly(**1**) was dissolved in CDCl₃ and heated at 65 °C. Additional olefinic peaks at 6.0–6.2 ppm emerged, which were tentatively assigned to conjugated olefins generated from ring-opening of cyclobutanes (Fig. S8†). Interestingly, the peak intensity of new olefins quickly saturated after 3 h of heating and remained unchanged after additional 37 h of heating at the same temperature. Further increasing the temperature to 90 °C for another 24 h did not result in much change in the peak intensity (Fig. S9†). This result implies that a fraction of cyclobutanes in the polymer are less thermally stable than the rest, which also agrees with the two overlapping exothermic peaks at different temperatures from the DSC analysis (Fig. S4†). To investigate whether the configuration of backbone olefins would influence the thermal stability of cyclobutanes, we synthesized a Z-olefin rich polymer using a Z-selective Grubbs catalyst[26] and examined the thermal stability using the same ¹H NMR analysis. Surprisingly, almost identical thermal decomposition profile was observed despite the distinct difference in backbone olefin configurations (Fig. S10†). At this point, the reason behind this unusual thermal behavior remains unknown.

Recently, Bielawski and coworkers reported poly(dewar benzene), which has the same divinyl cyclobutane backbone structure.[27] This polymer was also found to be unstable, but was stabilized after hydrogenation of the backbone olefins. Therefore, we hydrogenated the backbone olefins of poly(**1**) using tosylhydrazide to improve the thermal stability. Hydrogenation also simplifies the analysis of mechanically generated olefins by eliminating the formation of conjugated backbone olefins, which have complex configurations and broad ¹H NMR signals. Freshly prepared poly(**1**) was hydrogenated using tosyl hydrazide (5 equiv. to olefin) with added NEt₃. ¹H NMR analysis of the hydrogenated polymers (**P1-H** and **P2-H**) showed complete

disappearance of olefinic peaks and unnoticeable ring-opening of cyclobutane (Fig. S46†). Their GPC traces exhibited narrow-disperse peaks with the same distribution as the ROMP polymers and MWs close to the theoretical values (Fig. 1b, Table 1). The hydrogenated polymers showed significantly improved thermal stability with a T_d over 400 °C (Fig. 1c). DSC analysis showed that **P1-H** is amorphous with a T_g of 94 °C (Fig. S5†).

Hydrogenated poly(**1**) also exhibited excellent stability towards acidic or basic conditions. Treating their solutions with either 100 mM HCl or KOH resulted in no change in GPC traces (Fig. 3c) or ¹H NMR spectra (Fig. S13†) over multiple days. The absence of any labile linkages in both polymer backbone and side chain is attributed to the high chemical stability prior to the mechanoactivation of the polymers.

To study the mechanoactivation, we subjected a dilute solution of **P1-H** in THF (1 mg mL⁻¹) to pulsed ultrasonication. Aliquots removed at regular time intervals were analyzed by both GPC and ¹H NMR spectroscopy. The GPC traces showed a rapid decrease of the original polymer peak and appearance of lower MW peak (Fig. 2b). The M_n decreased steadily and reached an ultimate MW of 18.0 kDa after 480 min of ultrasonication. Sonicating a shorter polymer **P2-H** under the same conditions resulted in a similar ultimate M_n of 18.7 kDa. ¹H NMR analysis showed a continuous decrease in cyclobutane
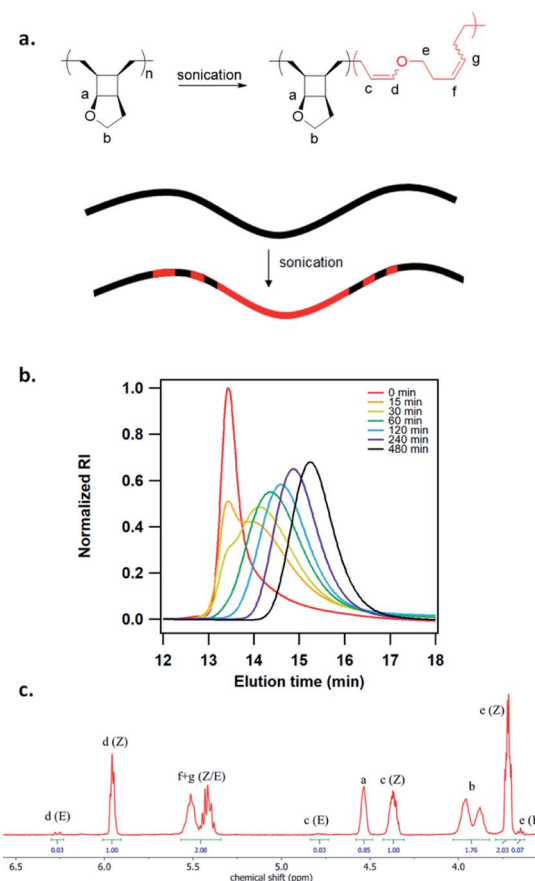

Fig. 2 (a) Mechanochemical activation of **P1-H** to generate poly(enol ether). (b) GPC traces of **P1-H** at different sonication times. (c) ¹H NMR spectrum of activated **P1-H** after 240 min of sonication.
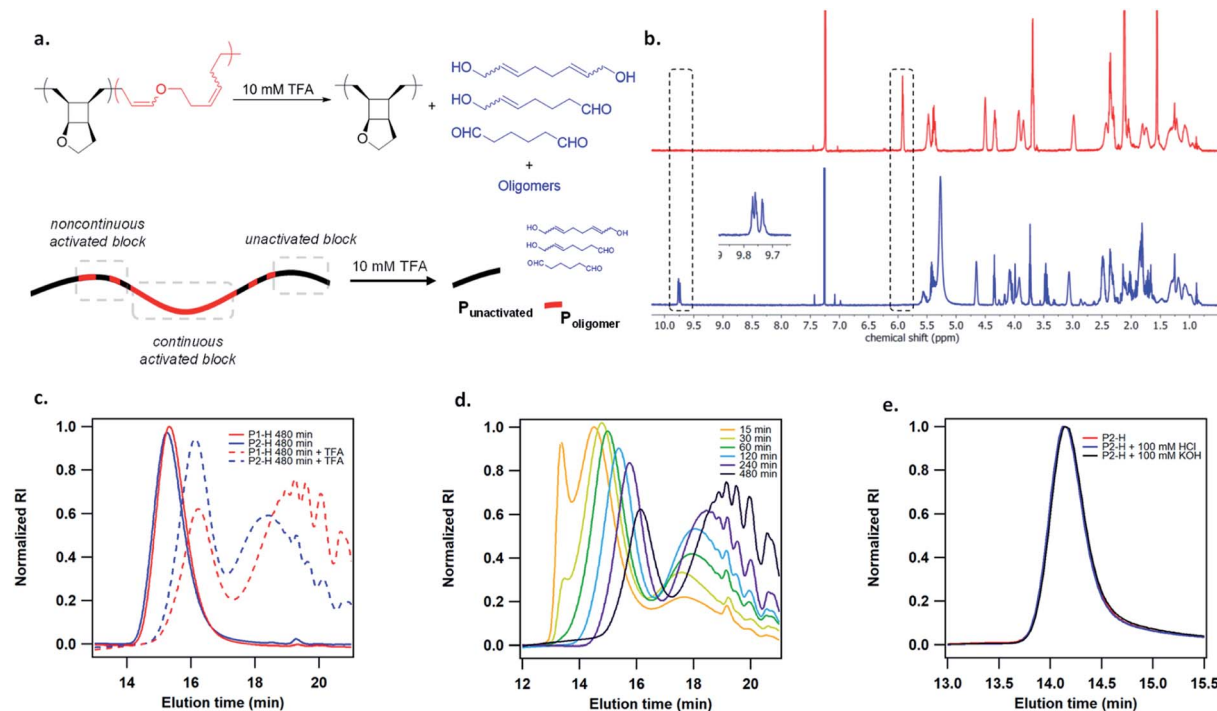
Fig. 3 (a) Acid degradation of mechanically activated polymer. (b) ^{1}H NMR spectra of mechanically activated poly(1) before (top, red trace) and after (bottom, blue trace) 10 mM TFA treatment. (c) GPC traces of hydrogenated poly(1) showing resistance to acidic and basic hydrolysis. (d) GPC traces of activated P1-H at different times after 10 mM TFA treatment. (e) Comparison of GPC traces of P1-H and P2-H after 480 min of sonication and 10 mM TFA treatment.

signals along with a concomitant increase in two sets of alkenyl peaks at the same intensity, corresponding to the generated enol ether olefin and the other olefin as assigned in Fig. 2c. The activation ratio increased steadily overtime and reached up to 65% and 55% for P1-H and P2-H, respectively, after 480 min of ultrasonication based on the ^{1}H NMR integrations (Fig. S14, S15, Tables S2 and S3†). These degrees of activation are notably higher than our other polymechanophore systems that were similarly synthesized by ROMP of mechanophore monomers but generated conjugated polymers,[21–24] which typically show a final degree of activation around 40%. The lower degree of activation observed in our other systems may be attributed to the variable extent of microscale aggregation and potentially occasional chemical crosslinking of the generated conjugated segments, which may disrupt the force transduction to some regions of the polymer strand. The absence of extended conjugation in the activated P1-H also gives them well resolved ^{1}H NMR signals, in contrast to the broad and partly suppressed signals for the mechanically generated conjugated polymers.

The generated poly(enol ether)s consisted of nearly all Z olefins with an E/Z ratio of 3 : 100 regardless of the MW and remained unchanged over the course of ultrasonication (Fig. 2c). The predominant formation of Z olefins represents stereochemical retention in the mechanochemical ring-opening. Interestingly, other studies of cyclobutane mechanochemical cycloreversion by Craig[28] and Wang[15] groups reported higher fractions of stereochemical inversion. The stereochemical distribution of the mechanochemically generated diene can

be ascribed to the instability of the diradical transition state upon the first bond scission and dynamic effect,[29,30] and warrants comprehensive computational studies. 22% and 28% mechanophore activation per scission cycle was achieved for P1-H and P2-H, respectively (Fig. S17†), agreeing with the previous report that shorter polymers are more selective in mechanophore activation over nonselective chain cleavage.[31]

The activated polymers after 480 min of sonication were then degraded by the addition of 10 mM TFA. ^{1}H NMR analysis showed the complete disappearance of enol ether signals as well as the appearance of multiple aldehyde peaks at 9.7–9.8 ppm (Fig. 3b), as expected from several aldehyde-containing degradation products at different MWs. Several small molecule hydrolysis products may be expected due to the regio-irregular placement of the pendent cyclic ether rings in the polymers (Fig. S21†). GPC analysis of the hydrolyzed polymer showed a bimodal distribution with a relatively narrow-disperse high MW peak representing the unactivated fraction of the polymer strand (P$_{unactivated}$), which is presumably located toward the ends of pre-activated polymer, and a low MW population corresponding to the generated oligomers and small molecules from hydrolysis(P$_{oligomer}$), which were formed due to the noncontinuous activation of mechanophore repeat units. Theoretically, the distribution of force on a polymer chain under elongational flow can be described using a bead-rod model, where force is maximal around the chain center and gradually decreases toward chain ends.[32] Presumably, mechanophores are activated more continuously under high forces
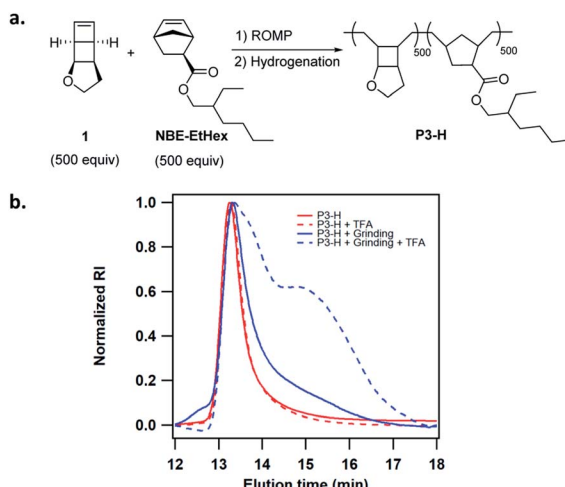
Fig. 4 (a) Synthesis of copolymer **P3-H**. (b) Changes of GPC traces of **P3-H** before and after grinding for 10 min, followed by treatment with 10 mM TFA in THF.

and less continuously as the force approaches activation threshold (Fig. 2a). Intriguingly, the M_n of both $\mathbf{P_{unactivated}}$ and $\mathbf{P_{oligomer}}$ decreased gradually over the course of sonication (Fig. 3d). Notably, the $\mathbf{P_{unactivated}}$ fraction of **P1-H** and **P2-H** after 480 min sonication had similar M_n of 9.6 and 11.4 kDa, respectively, despite their different original M_n of 141 and 63.1 kDa for the full-length polymers. However, most interestingly, the MW distribution of the $\mathbf{P_{oligomer}}$ fraction for these two samples were noticeably different (Fig. 3e). Longer **P1-H** resulted in shorter oligomers after degradation, indicating a shorter distance between the activated units or less discontinuous activation for the longer polymer.

We next attempted activation of poly(**1**) in the solid state. The facile copolymerization of **1** with substituted norbornenes provides a simple means to tune the solid state properties of the copolymers. Poly(**1**) is a glassy polymer with T_g of 94 °C. We copolymerized **1** with **NBE-EtHex** to lower T_g and generate more viscoelastic polymers (Fig. 4a). Copolymer **P3** of **1** with **NBE-EtHex** at 1 : 1 ratio was easily synthesized in low dispersity and controlled MW (Table 1). **P3** was completely hydrogenated using tosyl hydrazide without side reactions on the ester side chains as evidenced by ^{1}H NMR analysis (Fig. S25†). The hydrogenated copolymer **P3-H** showed a T_g of 56 °C (Fig. S26†). To demonstrate the solid state activation, we ground **P3-H** in a mortar for about 10 min. The GPC trace of ground **P3-H** showed slight tailing resulting from mechanical degradation of the polymer. 10 mM TFA was then added to **P3-H** before and after grinding. While the GPC trace for **P3-H** without grinding essentially remained unchanged, a considerable fraction of lower MW polymers was observed for the ground **P3-H** (Fig. 4b), suggesting the formation of hydrolysable enol ether linkages.

Conclusions

In summary, we have developed a new polymechanophore system that is hydrolytically robust but uncovers a large number of hydrolytically labile bonds in the polymer backbone under mechanical force. The mechanophore monomer can be rapidly polymerized by ROMP to yield homopolymers or copolymers. Hydrogenation of the backbone olefins of the ROMP polymers yielded saturated polymers with greatly enhanced thermal stability and excellent hydrolytic stability. The degradability of these polymers is turned on by mechanochemically transforming a previously non-degradable ether bond into a degradable enol-ether bond under stress applied by either sonication of the solution or grinding of the solid polymer. This design can impart additional chemical degradability to polymers beyond conventional mechanical chain scission and yield low MW oligomers and small molecules when under both stress and acidic conditions. We envision that the mechanophore monomer **1** can also be directly polymerized with other mechanophore monomers to allow facile degradation of the mechanically activated copolymers and facilitate detailed analysis of mechanochemical products in the future.

Conflicts of interest

There are no conflicts to declare.

Acknowledgements

Notes and references

1 M. M. Caruso, D. A. Davis, Q. Shen, S. A. Odom, N. R. Sottos, S. R. White and J. S. Moore, *Chem. Rev.*, 2009, **109**, 5755.

2 J. Li, C. Nagamani and J. S. Moore, *Acc. Chem. Res.*, 2015, **48**, 2181.

3 D. A. Davis, A. Hamilton, J. Yang, L. D. Cremar, D. Van Gough, S. L. Potisek, M. T. Ong, P. V. Braun, T. J. Martinez, S. R. White, J. S. Moore and N. R. Sottos, *Nature*, 2009, **459**, 68.

4 A. Piermattei, S. Karthikeyan and R. P. Sijbesma, *Nat. Chem.*, 2009, **1**, 133.

5 Y. Chen, A. J. Spiering, S. Karthikeyan, G. W. Peters, E. W. Meijer and R. P. Sijbesma, *Nat. Chem.*, 2012, **4**, 559.

6 A. L. Ramirez, Z. S. Kean, J. A. Orlicki, M. Champhekar, S. M. Elsakr, W. E. Krause and S. L. Craig, *Nat. Chem.*, 2013, **5**, 757.

7 M. B. Larsen and A. J. Boydston, *J. Am. Chem. Soc.*, 2013, **135**, 8189.

8 K. Imato, A. Irie, T. Kosuge, T. Ohishi, M. Nishihara, A. Takahara and H. Otsuka, *Angew. Chem., Int. Ed.*, 2015, **54**, 6168.

9 Y. Sagara, M. Karman, A. Seki, M. Pannipara, N. Tamaoki and C. Weder, *ACS Cent. Sci.*, 2019, **5**, 874.

10 T. Matsuda, R. Kawakami, R. Namba, T. Nakajima and J. P. Gong, *Science*, 2019, **363**, 504.

11 X. R. Hu, T. Zeng, C. C. Husic and M. J. Robb, *J. Am. Chem. Soc.*, 2019, **141**, 15018.

12 P. A. May and J. S. Moore, *Chem. Soc. Rev.*, 2013, **42**, 7497.

13 H. Staudinger, *Ber. Dtsch. Chem. Ges. A*, 1930, **63**, 921.

14 J. M. Lenhardt, M. T. Ong, R. Choe, C. R. Evenhuis, T. J. Martinez and S. L. Craig, *Science*, 2010, **329**, 1057.

15 T.-G. Hsu, J. Zhou, H.-W. Su, B. R. Schrage, C. J. Ziegler and J. Wang, *J. Am. Chem. Soc.*, 2020, **142**, 2100.

16 Y. Lin, T. B. Kouznetsova and S. L. Craig, *J. Am. Chem. Soc.*, 2020, **142**, 2105.

17 Y. Lin, T. B. Kouznetsova, C.-C. Chang and S. L. Craig, *Nat. Commun.*, 2020, **11**, 4987.

18 H. Shimomoto, T. Mori, T. Itoh and E. Ihara, *Macromolecules*, 2019, **52**, 5761.

19 J. D. Feist and Y. Xia, *J. Am. Chem. Soc.*, 2020, **142**, 1186.

20 X. Sui, T. Zhang, A. B. Pabarue, L. Fu and W. R. Gutekunst, *J. Am. Chem. Soc.*, 2020, **142**, 12942.

21 Z. Chen, J. A. M. Mercer, X. Zhu, J. A. H. Romaniuk, R. Pfattner, L. Cegelski, T. J. Martinez, N. Z. Burns and Y. Xia, *Science*, 2017, **357**, 475.

22 J. K. Su, J. D. Feist, J. Yang, J. A. M. Mercer, J. A. H. Romaniuk, Z. Chen, L. Cegelski, N. Z. Burns and Y. Xia, *J. Am. Chem. Soc.*, 2018, **140**, 12388.

23 J. Yang, M. Horst, J. A. H. Romaniuk, Z. Jin, L. Cegelski and Y. Xia, *J. Am. Chem. Soc.*, 2019, **141**, 6479.

24 J. Yang, M. Horst, S. H. Werby, L. Cegelski, N. Z. Burns and Y. Xia, *J. Am. Chem. Soc.*, 2020, **142**, 14619.

25 K. C. Nicolaou, C. K. Hwang, M. E. Duggan and K. B. Reddy, *Tetrahedron Lett.*, 1987, **28**, 1501.

26 B. K. Keitz, A. Fedorov and R. H. Grubbs, *J. Am. Chem. Soc.*, 2012, **134**, 2040.

27 J. Seo, S. Y. Lee and C. W. Bielawski, *Macromolecules*, 2020, **53**, 3202.

28 Z. S. Kean, Z. Niu, G. B. Hewage, A. L. Rheingold and S. L. Craig, *J. Am. Chem. Soc.*, 2013, **135**, 13598.

29 M. Wollenhaupt, C. Schran, M. Krupička and D. Marx, *ChemPhysChem*, 2018, **19**, 837.

30 Z. Chen, X. Zhu, J. Yang, J. A. M. Mercer, N. Z. Burns, T. J. Martinez and Y. Xia, *Nat. Chem.*, 2020, **12**, 302.

31 J. M. Lenhardt, A. L. Black Ramirez, B. Lee, T. B. Kouznetsova and S. L. Craig, *Macromolecules*, 2015, **48**, 6396.

32 A. Keller and J. A. Odell, *Colloid Polym. Sci.*, 1985, **263**, 181.